THE JOURNAL OF PHYSICAL CHEMISTRY A

 VOLUME 106, NUMBER 26, JULY 4, 2002

ARTICLES

ArF Laser Photodissociation Dynamics of 1,4-Pentadien-3-ol: Laser-Induced Fluorescence Observation of OH Rovibrational States

Pradyot K. Chowdhury

Radiation Chemistry & Chemical Dynamics Division, Bhabha Atomic Research Centre, Trombay, Mumbai−400 085, India

Received: February 7, 2002; In Final Form: April 19, 2002

On photoexcitation at 193 nm, the $^1(\pi, \pi^*)$ excited 1,4-pentadien-3-ol appears to be undergoing rapid internal conversion producing a highly energized ground electronic state, which is followed by dissociation to $CH_2{=}CH{-}CH{-}CH{=}CH_2$ (pentadienyl) and OH radicals as primary products. While the laser-induced fluorescence (LIF) showed that only 1.1% of the nascent OH ($X^2\Pi$) are produced in the vibrationally excited state with $v = 1$, there is no OH produced with $v = 2$. The rotational state distribution of OH is found to fit a Boltzmann distribution, characterized by a rotational temperature, T_{rot}, of 1250 ± 100 K for the $v = 0$ and T_{rot} of 1020 ± 100 K for the $v = 1$ vibrational states. By measuring the Doppler spectroscopy of the $v = 0$ and $v = 1$ states of OH, an average relative translational energy of the photofragments is found to be 41.8 ± 5.0 and 37.4 ± 5.0 kJ mol^{-1}, respectively. The real time formation of OH shows a dissociation rate constant of the 1,4-pentadien-3-ol to be (2.0 ± 0.4) × 10^7 s^{-1}. The above dissociation rate in relation to statistical Rice−Ramsperger−Kassel−Marcus (RRKM) theory suggests a resonance stabilization energy of the pentadienyl radical to be 70 kJ mol^{-1}.

1. Introduction

The dynamics of photodissociation following electronic excitation of small molecules have been studied extensively,[1−5] for which dissociation occurs on a time scale comparable to that of molecular vibrations (<1 ps). We have recently reported the instantaneous C−C bond dissociation from the Rydberg excited hydroxyacetone following absorption of a 193 nm photon,[6] whereas a slower dissociation of the C−O bond has been reported from the triplet surface,[7] on exciting the $^1(n, \pi^*)$ state of hydroxyacetone at 248 nm. Similarly, a nanosecond dissociation time scale of acetone on the excited singlet surface has recently been observed by Diau et al.[8,9] However, the long time required for molecular dissociation in the ground electronic state produced via internal conversion ensures that the energy acquired in the reactant is statistically distributed by intramolecular vibrational relaxation. In that case, the product flux is expected to be isotropic. The dissociation time scale of the molecule is expected to correspond to the predictions of the statistical unimolecular reaction rate theory. Our recent study[10] on the photodissociation of furfuryl alcohol is considered to be one such example of the molecular dissociation after internal conversion.

To the best of our knowledge, no UV−visible photochemical or thermal dissociation studies on 1,4-pentadien-3-ol (pentadienol) have been reported so far in the literature. The work reported here is the first study on the UV photochemistry of pentadienol to produce OH and pentadienyl radicals as the primary products. The dissociation of pentadienol may be considered as an intriguing system for the generation of OH in high yield. The OH radical is of great importance for the understanding of the complex mechanism involved in atmospheric chemistry modeling and combustion processes.

10.1021/jp0203649 CCC: $22.00
Published on Web 06/06/2002

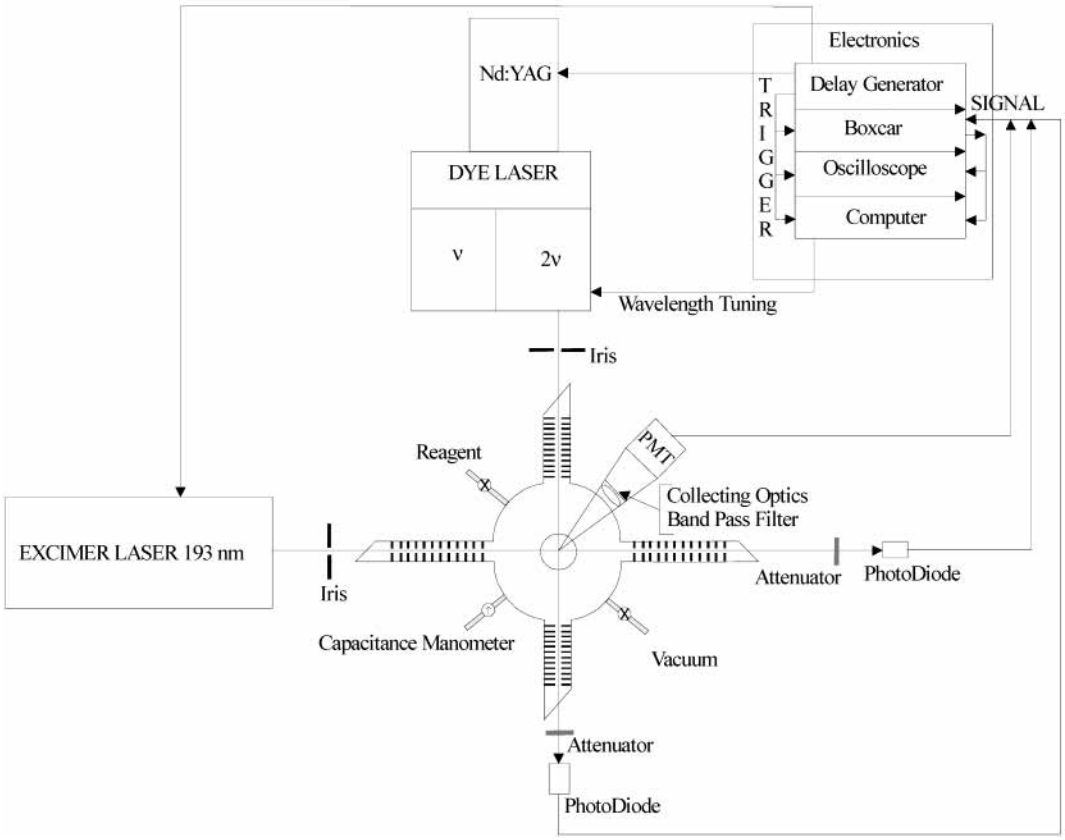

Figure 1. Experimental setup as described in the text.

Moreover, the OH radical has a rich rovibrational spectroscopy and is suitable for the determination of product energy distributions. Some information on the dissociation dynamics of pentadienol can be obtained from the nascent initial state distribution of the products, for example, OH(v,N,f), where v is the vibrational quantum number, N is the rotational quantum number, and f refers to one of the four OH fine structure levels.

2. Experimental Section

The schematic of the laser photolysis−laser-induced fluorescence setup (LP−LIF) used in the present study is shown in Figure 1. The details of the experimental procedures are given in our earlier publications,[6,10] and a brief account is as follows. The photolysis laser employed is an excimer laser (Lambda Physik model Compex-102, fluorine version) and the probe laser is Quantel dye laser with frequency doubling and mixing module (TDL 90) pumped by Quantel seeded Nd:YAG laser (model YG 980 E-20). The reaction chamber is made up of stainless steel with crossed right angle arms for photolysis and probe lasers. All of the arms are equipped with baffles and the windows are fixed at the Brewster angle to decrease scattering. The photolysis and the probe lasers intersect at the center of the reaction cell. The detection system views at right angle the intersection volume of photolysis and probe laser through the bottom arm window. The fluorescence is collected by a 38 mm diameter lens of focal length 50 mm and detected by a photomultiplier tube (PMT, Hamamatsu model R 928P). A band-pass filter (λ_{center} = 310 nm, fwhm = ±10 nm, $\%T_{310\ nm}$ = 10%) is placed between the collecting lens and the PMT to cut off the scattering from the photolysis laser. The fluorescence signal is gate integrated by a boxcar (SRS 250), averaged for 30 laser shots and fed into an interface (SRS 245) for A/D conversion. A Pentium II PC is used to control the scan of the dye laser via a RS232 interface and to collect data through a GPIB interface using the control and data acquisition program. To correct for the laser intensity fluctuations, both the pump and the probe lasers are monitored by photodiodes, and fluorescence intensities are normalized.

In the present work, the 1,4-pentadien-3-ol vapor is flowed through the reaction chamber at a flow velocity of approximately 10 cm/sec and photolyzed at 193 nm. The 1,4-pentadien-3-ol pressure is maintained at about 10 mTorr. The OH fragment is probed state-selectively by exciting the $A^2\Sigma \leftarrow X^2\Pi$ (0,0) transition of OH at 307−314 nm and the (1,1) transition of OH at 313−316 nm and followed by monitoring the total $A \rightarrow X$ fluorescence. The laser frequency was calibrated using the optogalvanic signal of a hollow-cathode lamp with an accuracy of ±0.3 cm^{-1}. The spectral resolution of the probe laser is 0.06 cm^{-1}. Both of the laser beams used are unfocused and attenuated further to prevent saturation. The measured LIF signal is found to be linearly proportional to the laser power. 1,4-Pentadien-3-ol (99% purity, Aldrich) was freeze−pump−thawed five times prior to use.

3. Results and Discussion

1,4-Pentadien-3-ol (pentadienol) undergoes a simple bond fission reaction producing two radicals, pentadienyl and OH, as follows:

$$CH_2{=}CH{-}CH(OH){-}CH{=}CH_2 \rightarrow CH_2{=}CH{-}CH{-}CH{=}CH_2 + OH$$

$$\Delta H^\circ = 317\ kJ\ mol^{-1}$$

The thermochemistry of pentadienol has not been reported in the literature; apparently, C−O is the weakest bond in this molecule. The C−O bond dissociation energy of $CH_2{=}CH{-}$

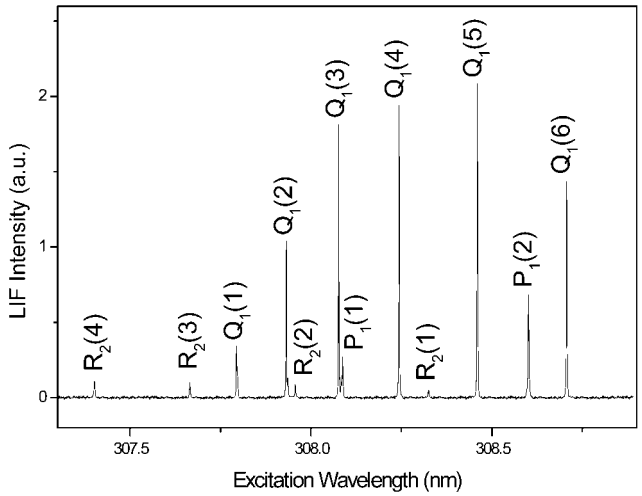

Figure 2. Portion of the laser-induced fluorescence (LIF) rotational excitation spectrum of OH radical formed in the irradiation of 1,4-pentadien-3-ol by an ArF excimer laser (20 ns, 150 mJ/pulse). The pentadienol pressure used is 10 mTorr, and the delay between the ArF and the dye laser is 100 ns. The spectral assignments are based on ref 15.

CH(OH)—CH═CH_2 is estimated to be about 317 kJ mol^{-1}, from the calculated heat of formation of pentadienol and pentadienyl radical to be −65[11] and 213[12] kJ mol^{-1}, respectively, and the reported[13] heat of formation of OH as 39 kJ mol^{-1}. However, one may find a pentadienol dissociation enthalpy change ($\Delta H°$) of about 308 kJ mol^{-1}, by using the heat of formation of pentadienyl radical calculated from the group additivity data of Dilling[14] to be 204 kJ mol^{-1}.

3.1. Rotational State Distribution of Nascent OH by LIF. The formation of OH radicals was observed in the irradiation of pentadienol by a pulsed ArF excimer laser. Typical LIF signals from OH exhibited simple exponential decays, with decay times consistent with OH $A^2\Sigma^+$-state measurements. A typical LIF spectrum of OH observed at a probe time of 100 ns after the excimer laser pulse and a pentadienol pressure of 10 mTorr is shown in Figure 2. At this pressure, the hard-sphere collision rate is 10^5 s^{-1} $molecule^{-1}$, which ensures that no collisional relaxation occurred within the probe time of 100 ns. The line assignment and nomenclature are based on the extensive spectroscopic work of Dieke and Crosswhite.[15] All of the peaks in Figure 2 correspond to transitions originating in the $X^2\Pi_i$ ($v = 0$) level. Normally, relative peak areas of the rotational lines of LIF signals were used to obtain relative OH densities. Conversion of the measured LIF signal S to a state-resolved OH($X^2\Pi$) population requires correction for variations in the intensity of both the ArF and probe lasers, I_{photol} and I_{probe}, as well as accurate values of the Einstein coefficients, B_{ik} for the k ← i transition at ν_{ik}.

$$P(v'',N'',f'',\lambda'') = \frac{S}{I_{photol} I_{probe} B_{ik} \nu_{ik}} \qquad (1)$$

The pump and probe laser intensity variation was monitored simultaneously with the LIF signal during spectral scan. Tabulated values of B_{ik} are used throughout.[16] Here, the energy of the probe laser (maximum energy about 10 mJ/pulse) was reduced by a factor of 1000 to ensure a linear response of the fluorescence to laser power. Conversion of the spectrum to micropopulations is obtained by dividing the state populations by their rotational degeneracy, $(2J'' + 1)$. A Boltzmann plot of rotational states, that is, $\ln[P(J)/(2J + 1)]$ vs E_R, the rotational energy of the state, is shown in Figure 3a. The straight line is the computer least-squares fit of the data, representing different Λ ($^2\Pi^+$, $^2\Pi^-$) and spin ($^2\Pi_{3/2}$, $^2\Pi_{1/2}$) states. They seem to have approximately the same Boltzmann distribution, characterized by a common rotational temperature (T_R) of 1250 ± 100 K. This measured distribution of initial rotational states corresponds to an average rotational energy in OH, $E_R = 10.4$ kJ mol^{-1}. A second set of experiments was carried out to cross check and determine $P(J)$ for OH($^2\Pi$) states, which gave an identical result for T_R.

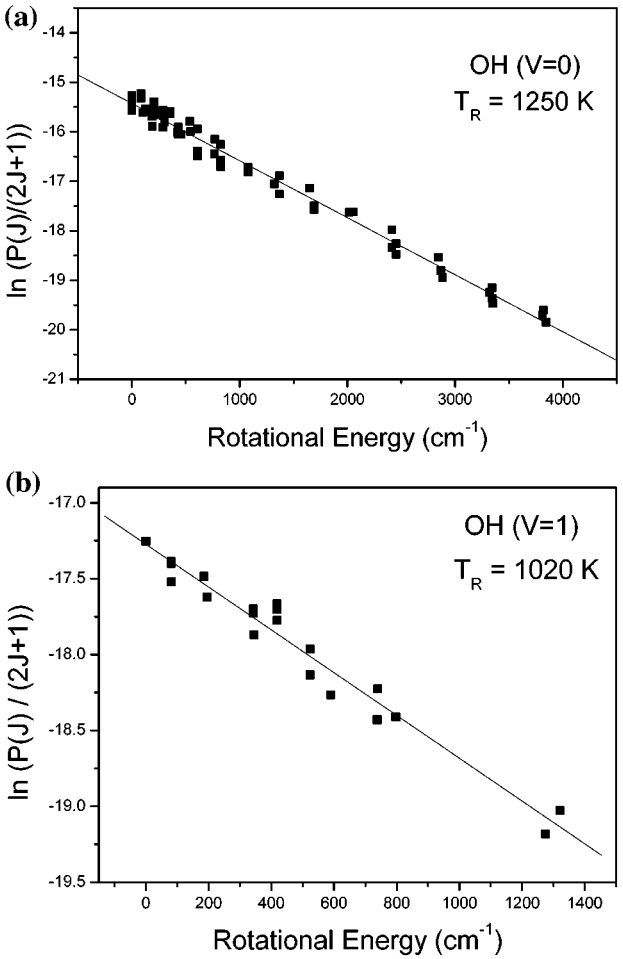

Figure 3. Boltzmann plot of the (a) $v = 0$ populations in various microstates of nascent OH. The distribution of four different spin and Λ doublet states of OH is characterized by a temperature $T_R = 1250 \pm 100$ K. Panel b shows a Boltzmann plot of the $v = 1$ populations in various microstates of nascent OH. The distribution of four different spin and Λ doublet states of OH is characterized by a temperature $T_R = 1020 \pm 100$ K.

To measure the rotational temperature of the OH produced in the $v'' = 1$ level, the LIF scan was continued through the (1,1) vibrational transition up to the P_1 (6) rotational line. A Boltzmann plot of rotational states, that is, $\ln[P(J)/(2J + 1)]$ vs E_R, the rotational energy of the state, is shown in Figure 3b. The straight line fit of the data, representing different Λ ($^2\Pi^+$, $^2\Pi^-$) and spin ($^2\Pi_{3/2}$, $^2\Pi_{1/2}$) states, seems to have approximately the same Boltzmann distribution, characterized by a common rotational temperature (T_R) of 1020 ± 100 K. This measured distribution of initial rotational states corresponds to an average rotational energy in OH, $E_R = 8.5$ kJ mol^{-1}. By integrating the population of the rotational states in the $v'' = 1$ and $v'' = 0$ bands, about 1.1% of the OH is found to be produced in the $v'' = 1$ state. This corresponds to a vibrational temperature of $T_V = 1150 \pm 100$ K.

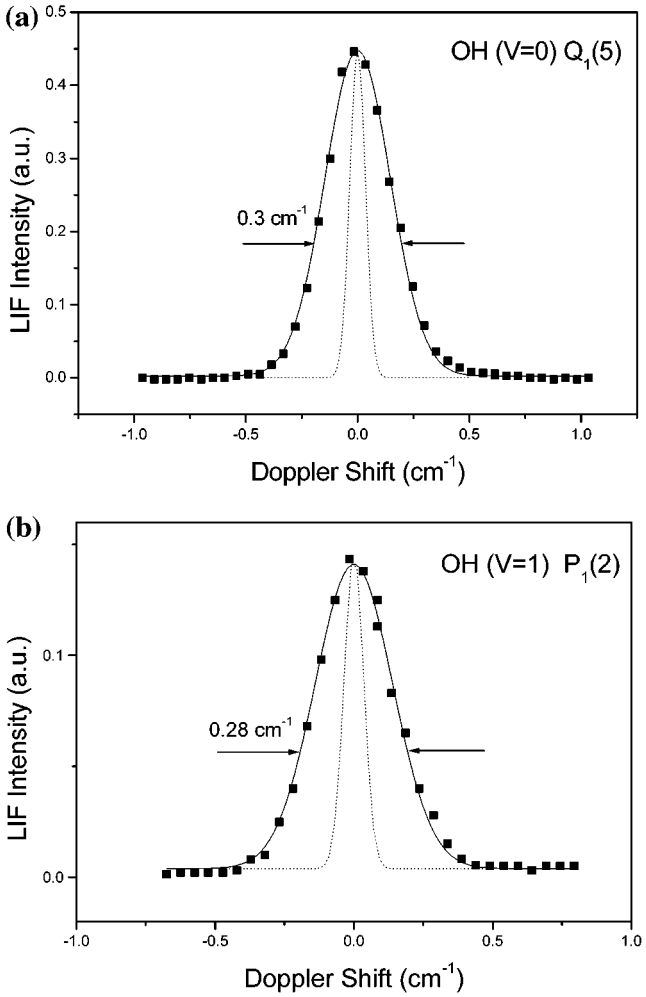

Figure 4. Doppler profile of (a) the $Q_1(5)$ rotational line of the (0,0) transition of OH in the spectrum. and (b) the $P_1(2)$ rotational line of the (1,1) transition of OH in the spectrum. The solid line drawn through the data points represents a Gaussian fit to the data points. The dotted line represents the instrument function (fwhm = 0.07 cm^{-1}).

3.2. Translational Energy of OH from Doppler Line Width. The component of OH fragment velocity along the probe laser propagation axis *z*, v_z, shifts the central absorption frequency ν_0 to ν by the following equation:

$$\nu = \nu_0(1 \pm v_z/c) \tag{2}$$

where *c* is the velocity of light. The line width and shape of the Doppler-broadened LIF line include contributions from the fragment molecular velocity, the thermal motion of the parent, and the finite probe laser line width. The peak profile for $Q_1(5)$ is shown in Figure 4a. All of the rotational lines are seen to exhibit the same line width within the experimental error. For a completely isotropic OH fragment velocity distribution, the deconvolution of the peak profiles with the instrumental function gives the Doppler width to be 0.29 ± 0.02 cm^{-1}. For the Maxwell−Boltzmann translational energy distribution, this corresponds to an average relative translational energy of 41.8 ± 5.0 kJ mol^{-1} in the center of mass coordinate of the photofragments, after due correction for the thermal energy of the parent. The OH velocity distribution is expected to be very broad because its recoil partner pentadienyl has high density of internal states. We have assumed a Gaussian profile for the velocity distribution, which fits quite well with the observed velocity distribution.

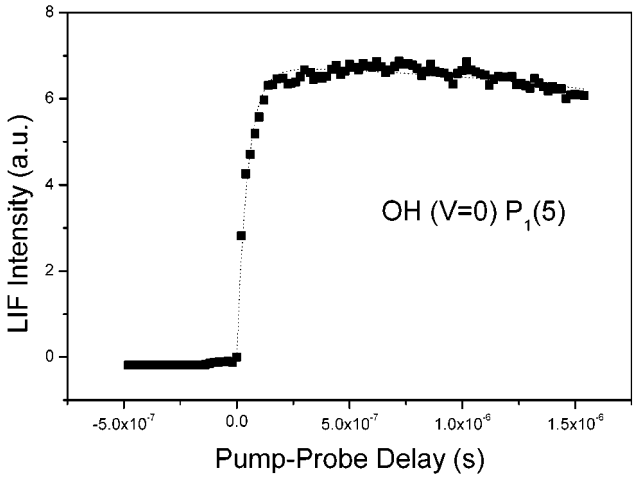

Figure 5. LIF intensity of OH generated in the dissociation of pentadienol as a function of the pump−probe delay. The pentadienol pressure is 10 mTorr and the ArF laser fluence is 0.1 mJ cm^{-2}.

To see the Doppler profile in the vibrationally excited OH, the peak profile for $P_1(2)$ of the (1,1) transition is scanned, which is shown in Figure 4b. This band shape also fits well with the Gaussian function, giving a Doppler width of 0.28 ± 0.02 cm^{-1}. For the Maxwell−Boltzmann translational energy distribution, this corresponds to an average relative translational energy of 37.4 ± 5.0 kJ mol^{-1} in the center of mass coordinate of the photofragments.

3.3. Kinetics of 1,4-Pentadien-3-ol Dissociation. The production of OH ($v'' = 0$) as a function of the delay time between the two lasers was obtained by monitoring the intensity of the $P_1(5)$ LIF signal as shown in Figure 5. The buildup of the signal was found to be rapid during a few hundred nanoseconds after the photolysis laser pulse, whereas a slower decay was observed up to 1.5 μs afterward. The first data point was taken at a probe laser fired 500 ns before the photolysis laser, and subsequent data points were taken at 20 ns intervals afterward, which are averaged over 100 pulses. The measurement was carried out at a pentadienol pressure of 10 mTorr and at an ArF laser fluence of 0.1 mJ cm^{-2}. Several other intense rotational lines, mainly the strong lines of the Q_1 and P_1 branch of the (0,0) transition, were also measured as a function of the delay. It was found that the time-dependent signal intensities were independent of the rotational lines probed (4 or 6). This suggests that no significant rotational relaxation occurs on the above time scale.

The fast buildup of the OH signal due to OH fragments generated in the dissociation of 1,4-pentadien-3-ol suggests that its dissociation rate (*k*) could be $>10^7$ s^{-1}. A slow decay is observed afterward because of the diffusion of the nascent OH fragments. The average dissociation rate constant, *k*, of pentadienol was computed by fitting the time-dependent data (Figure 5) to a function,

$$I(t) = A[(B/C)t^2][1 - \exp(-kt)] \tag{3}$$

where *A* is a fitting parameter, *B* is related to the pump and probe laser beam radii and *C* is related to the diffusion coefficient.[18] The dissociation rate constant of pentadienol has been obtained as (2.0 ± 0.4) × 10^7 s^{-1}.

In another study, the 193-nm ArF excimer laser radiation was varied from 10 to 100 μJ/pulse, and the OH LIF intensity of the $Q_1(3)$ rotational line was monitored as a function of the excimer laser fluence. The log−log plot of LIF signal vs

TABLE 1: Parameters Used in RRKM Calculations

vibrational wavenumbers, cm^{-1}	
1,4-pentadien-3-ol molecule	activated complex
3653, 3092(2), 3000(2), 2980, 2875(2), 1650(2), 1417, 1315(3)*, 1229(2)*, 1120, 1027, 980(2)*, 964(2), 885(4)*, 629(2), 562(2)*, 440(2)*, 290*, 206*, 95*, 76*	as for molecule except those with asterisk replaced by 1200(3), 1150(2), 1160(2), 700(4), 450(2), 300(2), 200, 194, 220, 146 and 1027 dropped to become reaction coordinate
	$\log[A\ (s^{-1})] = 14.6$ critical energy = 317 kJ mol^{-1} reaction path degeneracy = 1 ratio of adiabatic partition functions, $Q^{\dagger}/Q = 1.2$

photolysis energy yields a slope of 1.1 ± 0.1. This indicates that the OH radicals are produced in a single-photon process.

3.4. Evaluation of the Rate Constant Using Rice−Ramsperger−Kassel−Marcus (RRKM) Theory. The rate of formation of the nascent dissociation product, OH, from the highly energized pentadienol produced by fast internal conversion of pentadienol molecules excited by a 193-nm photon can be obtained by Rice−Ramsperger−Kassel−Marcus (RRKM) calculations. If the internal energy (E^*) of a molecule exceeds the dissociation energy, E_0, the molecule is capable of spontaneous decomposition to fragments. The unimolecular decomposition rate $k(E^*)$ in a RRKM approximation[17] is described by the expression

$$k(E^*) = \frac{gQ^{\dagger}G(E^{\dagger} = E^* - E_0)}{QhN(E^*)} \qquad (4)$$

where $N(E^*)$ is the density of states for the molecule at E^*. The term $G(E^{\dagger})$ is the sum of state of critical configuration up to an excess energy $E^{\dagger}$, g is the reaction path degeneracy, and $Q^{\dagger}/Q$ is the ratio of adiabatic partition functions. Sums and densities of states are calculated by using the Whitten−Rabinovitch method.[17] The threshold energy for the dissociation of pentadienol is taken as 317 kJ mol^{-1}. A frequency factor of $\log A(s^{-1}) = 14.6$ can be estimated by comparison with the unimolecular dissociation of benzyl alcohol,[18] which generates benzyl and OH radicals as products. The pentadienol vibrational frequencies are obtained from HF/6-311G** level calculation[19] (Gaussian 92) of structural optimization and normal modes, which are corrected with a factor of 0.89. The C−O stretching mode at 1027 cm^{-1} has become the reaction coordinate, and some of the vibrational frequencies are adjusted until agreement is reached between the A factor and the predicted entropy of activation. The frequencies taken for the activated complex and other parameters used in the RRKM calculations are given in Table 1.

The total energy of the 1,4-pentadien-3-ol molecule after absorbing a photon is $E_{tot} = h\nu + E_{th}$. The term E_{th} is the thermal energy of the molecule at room temperature, obtained as

$$\langle E_{th} \rangle = KT\sum(h\nu_i/(kT))/[\exp(h\nu_i/(kT)) - 1] \qquad (5)$$

where the ν_i terms are the vibrational frequencies of the molecule. Following rapid internal conversion after absorbing a 193.3-nm photon, the E_{tot} of pentadienol is 630 kJ mol^{-1}, which corresponds to a RRKM unimolecular dissociation rate constant of 2.0×10^7 s^{-1}. This dissociation rate is found to be in agreement with the experimentally measured value observed by our time-resolved pump−probe delay experiment. However, by repeating the same RRKM calculation with a lower threshold dissociation energy of 308 kJ mol^{-1}, a dissociation rate constant of pentadienol at 630 kJ mol^{-1} is found to be 3.8×10^7 s^{-1}, which is much higher than that of our experimental results.

3.5. Dissociation Energy Dynamics. The observation of 1.1% of the OH produced in the $\upsilon = 1$ corresponds to a vibrational temperature of $T_V = 1150 \pm 100$ K. This translates to an average vibrational energy in OH of $E_V = 0.5$ kJ mol^{-1}. The measured distribution of rotational states, characterized by a rotational temperature T_{rot} of 1250 ± 100 K at $\upsilon = 0$ and T_{rot} of 1020 ± 100 K at $\upsilon = 1$, corresponds to an average rotational energy of OH of $E_R = 10.4$ kJ mol^{-1}. The observation of OH translation by Doppler spectroscopy is found to fit with a Maxwell−Boltzmann velocity distribution, which corresponds to a release of an average translational energy of about 41.8 kJ mol^{-1} in the center of mass coordinate of the product fragments. When the above-mentioned energy associated with the rovibrational degrees of freedom of OH and overall translational energy for both the photofragments are subtracted from the available product energy, it gives us an internal energy of pentadienyl radical to be about 260.5 kJ mol^{-1}. This seems to be in agreement with a simple statistical model,[20] which suggests that about 261 kJ mol^{-1} remains as internal energy of the pentadienyl radical and 43.5 kJ mol^{-1} with the kinetic energy of the photofragments, from the 313 kJ mol^{-1} of excess energy available in the primary photodissociation. No significant selectivity for production of either fine structure state in OH-($^2\Pi$, $\upsilon'' = 0,1$) is observed. This may be due to the high density of vibrational states in pentadienol at the dissociation energy of 630 kJ mol^{-1}, which is about 10^{23} states/cm^{-1}. The redistribution of energy among such a high number of vibrational states during the tens of nanosecond time scale of the pentadienol dissociation suggests that the memory effect of the fine structure is lost.

3.6. Resonance Stabilization Energy of Pentadienyl Radicals. It has been reported[21] that the resonance stabilization energy (RSE) of the allyl radicals is in the range of 59−61 kJ mol^{-1}. In the pentadienyl radicals, the single unpaired electron is expected to be more extensively delocalize over all five carbon atoms, than that of the allyl radicals, in which delocalization is over three carbon atoms. However, the RSE of the pentadienyl radicals is reported to be marginally higher at 82 kJ mol^{-1} as shown by ab initio calculation[22] and 64,[23] 77, [24] and 71 [25] kJ mol^{-1} by experiment. In this study on the photodissociation of pentadienol at 193 nm, the real time formation of OH showed a dissociation rate constant of the 1,4-pentadien-3-ol to be 2.0×10^7 s^{-1}. The experimentally measured dissociation rate corresponds with the statistical RRKM calculated rate, with a threshold dissociation energy of pentadienol as 317 kJ mol^{-1}. In case of methanol dissociation to produce methyl and OH radicals, the C−O bond dissociation energy is computed from the recently reported[13] heat of formation values to be 387 kJ mol^{-1}. Thus, observation of a lower C−O bond dissociation energy of 317 kJ mol^{-1} in pentadienol than that of the methanol corresponds to a resonance stabilization energy of the pentadienyl radical to be 70 kJ mol^{-1}. This is close in agreement with the reported RSE of pentadienyl radicals by Doering et al. [25] using a different experimental technique.

4. Conclusions

The photodissociation of 1,4-pentadien-3-ol (pentadienol) has been demonstrated by excitation with an ArF excimer laser, generating pentadienyl radical and OH radical as primary products. The rovibrational spectroscopy of OH radical is studied by LIF. Most of the OH is formed in the ground vibrational

state, and only 1.1% is formed in the $v = 1$ state, giving a vibrational temperature of $T_{vib} = 1150 \pm 100$ K. The rotational state distribution of OH is found to fit a Boltzmann distribution, characterized by a rotational temperature, T_{rot}, of 1250 ± 100 K for $v = 0$ and T_{rot} of 1020 ± 100 K for $v = 1$ rotational states. No preferential OH formation in either spin doublets or Λ doublets could be observed. By analysis of the OH rotational Doppler line widths, the relative translational energy associated with the photofragments in the center-of-mass coordinate was found to be 41.8 ± 5.0 and 37.4 ± 5.0 kJ mol^{-1} for the $v = 0$ and $v = 1$ states of OH, respectively. The real time formation of OH showed a dissociation rate constant of the 1,4-pentadien-3-ol to be $(2.0 \pm 0.4) \times 10^7$ s^{-1}. The experimentally measured dissociation rate in relation to statistical RRKM theory suggests a resonance stabilization energy of the pentadienyl radical to be 70 kJ mol^{-1}. The results clearly indicate that on photoexcitation at 193 nm the $^1(\pi, \pi^*)$ excited 1,4-pentadien-3-ol undergoes rapid internal conversion to form a highly energized ground electronic state, which is followed by dissociation.

Acknowledgment. The author thanks Dr. T. Mukherjee and Dr. A. V. Sapre for their keen interest in this work. It is a pleasure to acknowledge the valuable discussions with Dr. J. P. Mittal and his kind support.

References and Notes

(1) Owrutsky, J. C.; Baronavski, A. P. *J. Chem. Phys.* **1999**, *110*, 11206.
(2) Kim, S. K.; Petersen, S.; Zewail, A. H. *J. Chem. Phys.* **1995**, *103*, 477.
(3) North, S. W.; Blank, D. A.; Gezelter, J. D.; Longfellow, C. A.; Lee, Y. T. *J. Chem. Phys.* **1995**, *102*, 4447.
(4) Nadler, I.; Mahgerefteh, T.; Reisler. H.; Wittig, C. *J. Chem. Phys.* **1985**, *82*, 3885.
(5) Zare, R. N. *Faraday Discuss. Chem. Soc.* **1986**, *82*, 391.
(6) Chowdhury, P. K.; Upadhaya, H. P.; Naik, P. D.; Mittal, J. P. *Chem. Phys. Lett.* **2002**, *351*, 201.
(7) Chowdhury, P. K.; Upadhaya, H. P.; Naik, P. D.; Mittal, J. P. *Chem. Phys. Lett.*, in press.
(8) Diau, E. W. G.; Kotting, C.; Zewail, A. H. *ChemPhysChem* **2001**, *2*, 273.
(9) Diau, E. W. G.; Kotting, C.; Zewail, A. H. *ChemPhysChem* **2001**, *2*, 294.
(10) Chowdhury, P. K.; Upadhaya, H. P.; Naik, P. D. *Chem. Phys. Lett.* **2001**, *344*, 298.
(11) Benson, S. W. *Thermochemical Kinetics*; Wiley: New York, 1976.
(12) Stein, S. E. *NIST Standard Reference Database 25: NIST Structure and Properties*, version 2.0; National Institute of Standard and Technology: Gaithersberg, MD, 1994.
(13) *CRC Handbook of Chemistry and Physics*, 80th ed.; Lide, D. R., Ed. CRC Press: Boca Raton, FL, 1999−2000.
(14) Dilling, W. L. *J. Org. Chem.* **1990**, *55*, 3286.
(15) Dieke, G. H.; Crosswhite, H. M. *J. Quant. Spectrosc. Radiat. Transfer* **1962**, *2*, 97.
(16) Chidsey, J. L.; Crosley, D. R. *J. Quant. Spectrosc. Radiat. Transfer* **1980**, *23*, 187.
(17) Robinson, P. J.; Holbrook, K. A. *Unimolecular Reactions*; Wiley-Interscience: New York, 1972.
(18) Chowdhury, P. K. *J. Phys. Chem.* **1994**, *98*, 13112.
(19) Frisch, M. J.; Trucks, G. W.; Head-Gorden, M.; Gill, P. M. W.; Wong, M. W.; Foresman, J. B.; Johnson, B. G.; Schlegel, H. B.; Robb, M. A.; Replogle, E. S.; Gomperts, R.; Andres, J. L.; Rahavachari, K.; Binkley, J. S.; Gonzalez, C.; Martin, R. L.; Fox, D. J.; Defrees, D. J.; Baker, J.; Stewart, J. J. P.; Pople, J. A. *Gaussian 92*, revision E.1; Gaussian, Inc.: Pittsburgh, PA, 1992.
(20) Campbell, R. J.; Schlag, E. W. *J. Am. Chem. Soc.* **1967**, *89*, 5103.
(21) Korth, H.-G.; Trill, H.; Sustmann, R. *J. Am. Chem. Soc.* **1981**, *103*, 4483.
(22) Fort, R. C., Jr.; Hrovat, D. A.; Borden, W. T. *J. Org. Chem.* **1993**, *58*, 211.
(23) Egger, K. W.; Benson, S. W. *J. Am. Chem. Soc.* **1966**, *88*, 241.
(24) Treniwith, A. B. *J. Chem. Soc., Faraday Trans. 1* **1980**, *76*, 266.
(25) Doering, W. v. E.; Kitagawa, T. *J. Am. Chem. Soc.* **1991**, *113*, 4288.